Biochimica et Biophysica Acta 1790 (2009) 1307–1313

Contents lists available at ScienceDirect

Biochimica et Biophysica Acta

journal homepage: www.elsevier.com/locate/bbagen

Proton motive force dissipation precludes interaction of microcin J25 with RNA polymerase, but enhances reactive oxygen species overproduction

Fernando G. Dupuy, María V. Niklison Chirou, Beatriz Fernández de Arcuri, Carlos J. Minahk, Roberto D. Morero *

Departamento de Bioquímica de la Nutrición, Instituto Superior de Investigaciones Biológicas (Consejo Nacional de Investigaciones Científicas y Técnicas—Universidad Nacional de Tucumán), Instituto de Química Biológica "Dr. Bernabe Bloj," Chacabuco 461. San Miguel de Tucumán T4000ILI, Argentina

ARTICLE INFO

Article history:
Received 27 February 2009
Received in revised form 7 July 2009
Accepted 8 July 2009
Available online 16 July 2009

Keywords:
Microcin
Reactive oxygen species
2,4 DNP
Peptide uptake
E. coli

ABSTRACT

Background: Microcin J25 targets the RNA polymerase as well as bacterial membranes. Because there is scarce information on the relationship between the uptake and the activity, a fluorescent microcin J25-derivative was used to further characterize its mechanism of action.
Methods: MccJ25 I13K was labeled with FITC and its uptake by sensitive cells was assessed by fluorescence measurements from supernatants of MccJ25-*Escherichia coli* suspensions. The interaction of the peptide with bacterial membranes was investigated by fluorescence resonance energy transfer. Oxygen consumption was measured with Clark-type electrode. RNA synthesis was evaluated *in vivo* by incorporation of [^{3}H]uridine. ROS production was assayed by measuring the fluorescence emission of the ROS-sensitive probe 5(and 6)-carboxy-2',7'-dichlorodihydrofluorescein diacetate.
Results: The protonophore 2,4-dinitrophenol decreased 80% of the MccJ25 uptake and prevented inhibition of transcriptional activity, the antibiotic intracellular target. On the other hand, peptide binding to bacterial membranes was not affected and antibacterial activity remained nearly unchanged. Proton gradient dissipation by protonophore accelerated cell oxygen consumption rates and enhanced MccJ25-related reactive oxygen species overproduction.
General significance: The deleterious reactive oxygen species would be produced as a consequence of the minor fraction of MccJ25 that interacts with the bacterial plasma membrane from the periplasmic side. These results show the first evidence of the mechanism underlying ROS production in sensitive bacteria.

1. Introduction

Microcin J25 (MccJ25) is a plasmid-encoded 21 amino acid antibiotic peptide with a distinctive lasso-structure [1–4]. It is produced by the *Escherichia coli* strain AY25 with the characteristic of being active against *E. coli*, *Salmonella enteritidis* and *Shigela* strains [2,5,6]. It was demonstrated that the target in *E. coli* is the RNA polymerase subunit β' [2,6,7]. However, it was also shown that MccJ25 inhibits the respiratory enzymes of plasma membrane in *S. enteritidis* serovar Newport, suggesting a dual mechanism of action [8]. This effect was also described in *E. coli*, where it was shown to be mediated by superoxide anion production [9].

Although the mechanism of action of MccJ25 was described in great detail, little is known about the relationship between the uptake of this peptide and its activity. The lack of tryptophan or easily derivatizable reactive groups, such as SH— and NH_2, makes uptake measurement a difficult task.

In this paper, a lysine-containing MccJ25 variant (MccJ25 I13K) was labeled with fluorescein isothiocyanate and the incorporation into bacterial cells as well as the effect of this peptide on its molecular targets were studied. Diminished uptake rate of the peptide into cells was observed by dissipating the protonic gradient with the protonophore 2,4 dinitrophenol (2,4 DNP), however, antimicrobial activity was not abolished. An alternative pathway of MccJ25 action in bacterial cells is discussed.

2. Materials and methods

2.1. Bacterial strains, media and growth conditions

In the present study we used *E. coli* AB1133 strain, provided by Coli Genetic Stock Center, and *E. coli* AB1133 (pGC01) and *E. coli* SBG 231 (*E. coli* AB259 *rpoC T931I*, MccJ25^r) which belonged to our microbial strain collection [9]. Unless otherwise indicated, strains were grown in Luria Bertani (LB, Sigma) liquid media at 37 °C with shaking.

The experiments made use of buffer salts and general reagents of the highest Sigma available commercial forms. N-lissamine rhodamine

* Corresponding author. Fax: +54 381 4248921.
E-mail address: rdmorero@fbqf.unt.edu.ar (R.D. Morero).

0304-4165/$ – see front matter © 2009 Elsevier B.V. All rights reserved.
doi:10.1016/j.bbagen.2009.07.006

B sulfonyl Dihexadecyl Phosphatidylethanolamine (RhoPE) >98% and 1,2-Dimyristoil-*sn*-Glycero-3-Phosphoethanolamine >99% (DMPE) were obtained from Avanti Polar Lipids. 5(and 6)-carboxy-2′,7′-dichlorodihydrofluorescein diacetate (COOH-H_2DCFDA) was purchased from Molecular Probes-Invitrogen.

2.2. Peptides sensitivity tests

Antibiotic activity of the peptides was assayed by spotting 10 µl of two-fold serial dilutions of peptide onto LB plates containing 1.6% agar, dried and overlaid with 4 ml 0.6% agar containing 10 µl of a stationary phase culture of AB1133 cells. Minimal inhibitory concentration (MIC) was taken as the highest dilution tested that produced a visible halo of growth inhibition. The effect of 2,4 DNP on peptides antibacterial activity was studied by adding 200 µM of the protonophore to both LB plates and the top agar layer.

Antibiotic activity in liquid media was also assayed by performing growth curves of AB1133 cells by seeding 10 ml of either LB or minimal salts M9 broth with 10 µl of a stationary phase culture. Evolution of the turbidity due to the increase of the bacteria number was followed by light dispersion at 590 nm in a Gilford 250 spectrophotometer. We assayed the effect of MccJ25 and the protonophore 2,4 DNP on bacterial growth by adding the corresponding MIC concentrations of MccJ25 and 200 µM 2,4 DNP to the medium.

2.3. Mutagenesis and peptides purification

To obtain the MccJ25 mutant, the plasmid pTUC342 carrying the *mcjA* gene under its own promoter was used. The modified plasmid was constructed by PCR technique with the appropriate primers and the mutation was confirmed by DNA sequencing. The strain *E coli* SBG231 was transformed with the plasmid pTUC342 carrying the mutated *mcjA* gene and the compatible plasmid pTUC341 as well, containing the *mcjBCD* genes required for synthesis and export of the antibiotic [10,11]. Both native MccJ25 and the mutated peptide carrying a substitution of Lys instead of Ile at the position 13 (MccJ25 I13K) were purified from 2-litre culture of strain SBG231, harbouring the corresponding plasmids as previously described [12]. The purity of the peptides was evaluated by analytical high performance chromatography in two different configurations of a Gilson HPLC system as follows: 20 µl of a 0.1 mg ml^{-1} solution of either MccJ25 or its variant, MccJ25 I13K, were loaded either on a µBondapak C18 column (10 µm, 3.9×300 mm — Waters) and eluted in a linear gradient from 20 to 80% (v/v) methanol in trifluoroacetic acid (TFA) 0.1% (v/v), or on a X-Terra MS C8 column (5 µm, 4.6×250 mm — Waters) and eluted in a linear gradient from 0 to 60% (v/v) acetonitrile in 0.1% TFA (v/v). Both MccJ25 and MccJ25 I13K peptides purified in our laboratory eluted as a single peak at the previous analytical chromatography systems.

2.4. Peptide labeling

The peptide MccJ25 I13K was labeled by coupling the lysine ε-amine group with the amine reactive probe fluorescein isothiocyanate (FITC). The labeling reaction was performed in 100 mM borate buffer, pH 8.0, containing a peptide:FITC ratio of 1:3 (w/w). After two hours at 25 °C in the dark, the mixture was loaded on a C8 cartridge, washed with excess of water and 30% (v/v) methanol in H_2O until no fluorescein was detectable in the eluate. The labeled peptide was then eluted with methanol and the solvent removed under vacuum in a rotary evaporator (Rotavapor®, Büchi, Switzerland). Finally, a re-purification on a C18 column was performed on a Gilson HPLC system using a linear gradient of 50 mM KH_2PO_4 pH 6.4 (Solvent A) and methanol (Solvent B).

2.5. Peptide uptake assay in intact cells

After growing at 37 °C to late exponential phase ($OD_{590}=0.8$), bacteria were harvested by centrifugation at 4 °C, washed twice with 20 mM Tris–HCl, pH 7.6, 100 mM NaCl, 1 mM EDTA, supplemented with 0.2% (w/v) glucose and resuspended at an $OD_{590}=4.0$ in the same medium. 1.5 µM of fluorescein-labeled MccJ25 I13K was added to the bacterial suspension (1 ml), the mixture was vortexed and incubated in darkness at 37 °C. At appropriate times, aliquots (100 µl) were taken and the supernatants were collected after centrifugation for 5 min at 10,000 ×*g*. The fluorescence emission was determined at 520 nm in the collected supernatants by exciting at 490 nm in an ISS-PC1 photon counting spectrofluorometer. The uptake of the fluorescein-labeled MccJ25 variant was calculated as follows:

$$\text{Uptake}(\%) = \frac{F_t}{F_0 - F_t} \times 100\ ,$$

where F_t is the intensity of the fluorescence emission at time "*t*" and F_0 is the intensity of the fluorescence emission of a control tube with no bacteria.

A displacement assay was performed by pre-incubating cells with MccJ25 before adding the labeled peptide, in order to confirm that the decrease of the residual fluorescence in supernatants was indeed due to the incorporation of the fluorescein-derivatized microcin by bacterial cells.

2.6. MccJ25 binding to isolated bacterial membranes

500 ml *E. coli* AB1133 culture was harvested in late exponential phase. Cells were washed twice with 30 mM Tris–HCl, pH 8, and spheroplasts were prepared essentially as described by Yamato et al. [13]. Thereafter, right-side out vesicles were obtained by hypotonic lysis following the protocol described by Tsuchiya [14]. Vesicles (1 mg protein) were fused by freeze–thaw cycles with 1 mM liposomes made of DMPE, then fused vesicles were sonicated 15 min at 4 °C. Homogeneous vesicle suspension was left undisturbed for 1 h at 4 °C prior to the experiment.

Right-side out vesicles were energized with 5 mM D-lactate and incubated with 1.5 µM fluorescein-labeled MccJ25 I13K in the presence or absence of 100 µM 2,4 DNP. After 30 min of incubation, vesicles were centrifuged at 150,000 ×*g* for 30 min. Pellets were gently resuspended in 100 µl 50 mM potassium phosphate buffer, pH 6.6 and fluorescence spectrum was analyzed from 500 nm to 600 nm ($\lambda_{exc}=470$ nm). The vesicles were able to generate a proton motive force when energized with D-lactate, as it was confirmed by using the potential-sensitive probe $DiSC_3$ [5,15] (data not shown). For experiments of energy transfer by fluorescence resonance (FRET), RhoPE was directly injected to membrane vesicles from an ethanolic solution at 0.1% w/w final concentration.

2.7. Transcription assays

In vivo RNA synthesis was determined essentially as described previously [7], that is, *E. coli* AB1133 was grown at 37 °C in 5 ml of M9 minimum medium supplemented with 1 mM $MgSO_4$, 1 µg thiamine ml^{-1} and 0.2% (w/v) glucose up to $OD_{590}=0.2$. Uridine and, when indicated, 2,4 DNP were added at final concentrations of 2 µg ml^{-1} and 200 µM, respectively, and then incubated in the presence or absence of 10 µM MccJ25 for 20 min at 37 °C. After preincubation, 740 Bq [^{3}H]uridine ml^{-1} was added and 0.5 ml samples were taken at 0, 20, 40 and 60 min. Transcription was stopped by adding 1.5 ml of 10% cold trichloroacetic acid (TCA). Incorporation of [^{3}H] uridine in the presence of azide was used as a negative control. The reactions were filtered through 0.45 µm filter pore size (HAWP02500 Millipore) and membranes were washed

with 1 ml 2% cold TCA, dried overnight at 45 °C and mixed with liquid scintillation cocktail for radioactivity counting on a Beckman LS1801 system.

To evaluate if fluorescein-labeled MccJ25 I13K retained the MccJ25 capability of inhibiting the bacterial RNA polymerase activity, an *in vitro* transcription assay was done by using purified RNA polymerase holoenzyme (σ saturated, Epicentre Biotechnologies). The reaction was initiated by the addition of 1 U of the holoenzyme to mixture assays (25 μl) containing 2 μg of purified plasmid pBR322, 2 mM DTT, 250 μM ATP, 250 μM GTP, 250 μM CTP and 140 Bq [^{3}H] UTP ml^{-1}, in 50 mM buffer Tris–HCl pH 7,5, 10 mM $MgCl_2$ and 0.01% Triton X100. The reaction was allowed to proceed for 15 min and stopped with 1 ml 10% cold TCA and passed through glass fiber filters (Millipore type APFC). Filters were dried overnight at 45 °C and mixed with liquid scintillation cocktail for radioactivity counting.

2.8. O_2 consumption

Oxygen consumption was measured with a Clark-type electrode in 2-ml stirred sample chambers according to Schurig-Briccio et al. [16]. Electrodes were calibrated by saturating with oxygen sample chambers by bubbling air. Bacterial cells grown at 37 °C up to late exponential phase (OD_{590} nm = 0.8) in a minimum salts media supplemented with glucose were harvested by centrifugation at 4 °C, washed twice with 20 mM Tris–HCl, pH 7.4, 100 mM NaCl, 1 mM EDTA and resuspended at OD_{590} = 0.2. The assay was started by addition of glucose as carbon source at 0.2% (w/v) final concentration. The residual dissolved oxygen in sample chamber was expressed as a percentage of the dissolved oxygen in buffer at saturation and plotted as a function of time. Consumption rates were calculated from the slopes of the recorded lines.

2.9. Measurement of radical species generation in cells

Intracellular oxidation of the fluorescein derivative 5(and 6)-carboxy-2′,7′-dichlorodihydrofluorescein diacetate by reactive oxygen species was measured [17]. The MccJ25-sensitive strain *E. coli* AB1133 was grown at 37 °C in M9 minimum medium supplemented with 1 mM $MgSO_4$, 1 μg thiamine ml^{-1} and 0.2% (w/v) glucose to mid-exponential phase (OD_{590} = 0.5), harvested at 9000 ×*g* at 4 °C, washed twice with buffer 20 mM Tris–HCl pH 7.8, 100 mM NaCl, 1 mM EDTA and resuspended in the same buffer at OD_{590} = 0.1. Cells were incubated with 5 μM COOH-H_2DCFDA in darkness at 37 °C for 30 min. Non-incorporated probe was removed from the media by pelleting and resuspending the cells at the same volume with fluorescent probe-free buffer. When indicated, probe-loaded cells were preincubated with 200 μM 2,4 DNP or with 250 μM carbonyl cyanide 3-chlorophenylhydrazone (CCCP) for 20 min. Respiratory chain inhibitor cyanide was added at 1 mM final concentration 20 min before measurements began. Fluorescence emission of the probe-loaded cells at 37 °C under stirring was recorded as a function of time in an ISS-PC1 spectrofluorometer equipped with a temperature controlled sample holder. Excitation and emission wavelengths were set at 485 nm and 520 nm, respectively.

3. Results

3.1. Relationship between uptake and antibacterial activity

Fluorescein-labeled MccJ25 I13K decreased RNA polymerase activity in an *in vitro* assay up to 30% with respect to a control reaction with no peptide. MccJ25 at equal concentrations (10 μM) produced 40% of enzyme inhibition. The derivatized microcin showed also antimicrobial activity toward *E coli* AB1133 (MIC = 1,2 μM), although this value was higher than MIC of native MccJ25 (0,2 μM).

The fluorescein-labeled MccJ25 variant was employed for studying the kinetics of the peptide incorporation into living cells by measuring the decrease of the fluorescence at 520 nm in the supernatant of the strains treated with the labeled antibiotic (Fig. 1). To assess the significance of the peptide uptake on the antibiotic activity, we determined the minimal inhibitory concentration (MIC) of MccJ25 toward the same strains as well as the inhibition of oxygen consumption and transcriptional activity inhibition induced by the peptide (Table 1). Almost 70% of the labeled peptide was taken up from the solution by the sensitive *E. coli* strain AB1133 during the first 30 min. This strain transformed with pGC01 plasmid, which overexpresses the MccJ25 outer membrane receptor FhuA, incorporated the peptide at higher rates. Consequently, the antibiotic activity of MccJ25 was enhanced, as revealed by the decrease of the MIC from 0.24 to 0.02 μM, the inhibition of transcription and the augmented effect on the respiratory chain, which was observed upon increasing the antibiotic intracellular accumulation. The natural resistant strain SBG231, in which RNA polymerase is not inhibited by MccJ25 because of the substitution of Thr931 for Ile at the subunit β', which precludes binding of MccJ25 to the enzyme [7,18], was also able to take up the fluorescein-labeled peptide at similar levels of the sensitive strain AB1133, although at slightly slower rate (Fig. 1 and Table 1). Deleterious treatment of the cell with 10 mM azide and heat abolished microcin incorporation, indicating that peptide incorporation was indeed an active process (not shown). Pre-treatment of cells with 0.5 μM MccJ25 inhibited the uptake of the labeled peptide at 5% levels (Fig 1).

3.2. Effect of 2,4 dinitrophenol on the MccJ25 activity

Because the energy required by FhuA at the outer membrane is transduced by the TonB–ExbB–ExbD complex at the cytoplasmic membrane, which uses the proton motive force [19], the effect of the protonophore agent 2,4 DNP on the transport and antibiotic activity of MccJ25 was analyzed. The addition of 200 μM 2,4 DNP in the growth media delayed the bacterial growth, but identical OD_{590} was reached at the stationary phase (Fig. 2). The uptake of the peptide was severely inhibited in the presence of the uncoupling agent (Fig. 1). In fact, an uptake of about 20% could be measured in the presence of the

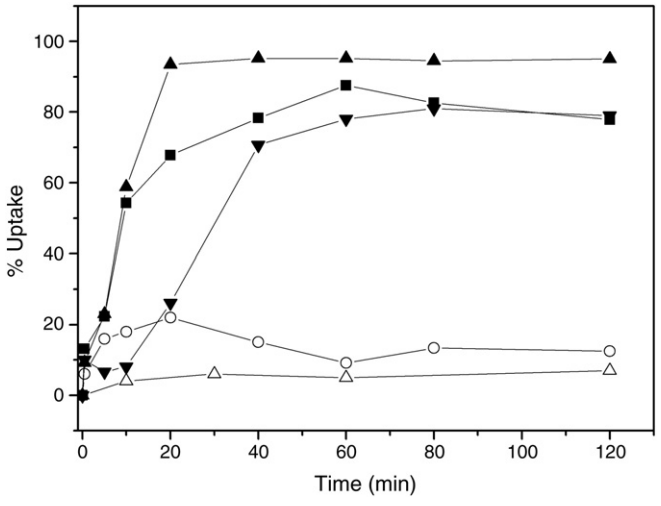

Fig. 1. Uptake of fluorescein-labeled MccJ25 I13K by different *E. coli* strains. 1.5 μM fluorescein-labeled MccJ25 I13K was added to the indicated bacterial strain suspended in 20 mM Tris–HCl, pH 7.6, 100 mM NaCl, 1 mM EDTA, supplemented with 0.2% glucose. The mixture was incubated at 37 °C in darkness. At appropriate times, the incorporation was stopped by centrifugation and the fluorescence emission at 520 nm was determined in the supernatant. Symbols: *E. coli* AB1133, (■); *E. coli* SBG231 (▼); *E. coli* AB1133 pGC01 (▲); *E. coli* AB1133 plus 200 μM 2,4 DNP (○); *E coli* AB1133 plus 0.5 μM MccJ25 (△). Excitation wavelength was set at 490 nm.

Table 1
Relationship between the uptake and antibiotic activity of MccJ25.

Strain	MIC (μM)	Oxygen consumption inhibition (%)	RNA polymerase inhibition (%)	Uptake (%)
E. coli AB1133	0.24	2.8 ± 1.1[a]	52.3 ± 7.2[a]	70
E. coli AB1133 pGC01	0.02	29.0 ± 4.1	55.8 ± 6.2	90
E. coli SBG231	>500	2.9 ± 1.1	No inhibition	70

[a] The results are expressed as mean ± SD of five independent experiments.

protonophore agent, indicating that a minor fraction of the antibiotic may be incorporated in an energy-independent manner.

Surprisingly, the inhibition of the uptake of MccJ25 induced by 2,4 DNP did not abolish antibiotic activity. As it is depicted in Fig. 2, when growth medium was supplemented with MccJ25 at inhibitory concentrations (MIC = 0.2 μM), the beginning of the exponential phase of the bacterial growth was further delayed, probably as a result of the combined action of the antibiotic peptide and the protonophore. At the stationary phase, however, the presence of 2,4 DNP and MccJ25 readily impaired the bacterial growth of *E. coli* AB1133, as OD_{590} values significantly lower than the MccJ25-lacking control cultures were observed. The persistent activity of MccJ25 in the presence of 2,4 DNP was also observed in solid media, although in this case MIC increased slightly from 0.2 μM in absence of 2,4 DNP to 0.8 μM in presence of 2,4 DNP (data not shown).

3.3. MccJ25 bacterial membranes binding

As several reports have previously shown the capability of MccJ25 to interact with membranes [8,12,20], we next investigated whether the remaining 20% of peptide uptake not inhibited by the uncoupling agent 2,4 DNP was bound to the bacterial envelope. We found that fluorescein-labeled microcin co-sedimented with bacterial membranes of AB1133 strain when the peptide-treated cells were sonicated and centrifuged at 100,000 ×*g*, either in absence or presence of 2,4 DNP (data not shown).

Since bacterial envelopes produced after sonication may represent a complex mixture of inner and outer membranes as well as peptidoglycan, the binding of the peptide to membrane was assayed in energized membrane vesicles prepared from lysed spheroplasts derived from AB1133 cells. As depicted in Fig. 3, a distinct fluorescence spectrum could be observed in the membrane vesicles indicating that microcine co-sedimented with these structures as well.

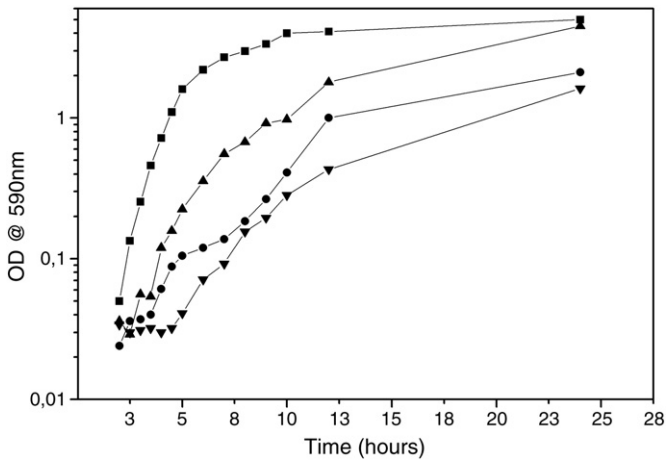

Fig. 2. Effect of 2,4 DNP on the MccJ25 activity. *E. coli* AB1133 alone (■) and in the presence of either 0.2 μM MccJ25 (●), 200 μM 2,4 DNP (▲), or 0.8 μM MccJ25 plus 200 μM 2,4 DNP (▼) was grown in M9 medium. Growth was monitored by measuring OD_{590} for 24 h.

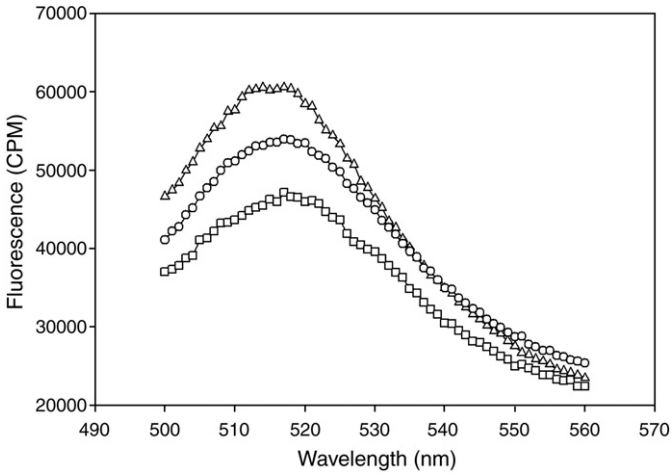

Fig. 3. Binding of MccJ25 to membrane vesicles. Membrane vesicles derived from *E. coli* AB1133 cells loaded with RhoPE were obtained as described in Materials and methods and energized with 5 mM D-lactate. Vesicles incubated with 1.5 μM fluorescein-labeled MccJ25 I13K in the absence (○), and in the presence of 200 μM 2,4 DNP (□) were centrifuged at 100,000 ×*g* and resuspended in 0.1 ml. Control experiment (△) was performed incubating fluorescein-labeled MccJ25 I13K with membrane vesicles lacking RhoPE. Fluorescence emission of the samples excited at 470 nm was recorded between 500 and 680 nm. The spectra are representative of 3 independent experiments.

Furthermore, when the labeled phospholipid RhoPE was added to vesicles, the fluorescence emission of the peptide decreased, indicating that a fluorescein to rhodamine energy transfer occurred. This result suggested us that the peptide was indeed closely associated with membrane-anchored RhoPE at the bacterial membrane. The binding to membrane was not apparently inhibited by the protonophore 2,4 DNP according to this experimental approach, in contrast to intracellular accumulation, as it was demonstrated before.

3.4. Effect of 2,4 dinitrophenol on the MccJ25 targets

It is known that besides RNA polymerase inhibition, MccJ25 acts on the respiratory enzymes activity and the bacteria plasma membrane [9]. Therefore, we tested how the activity on both molecular targets was affected upon treatment with 2,4 DNP. RNA polymerase activity

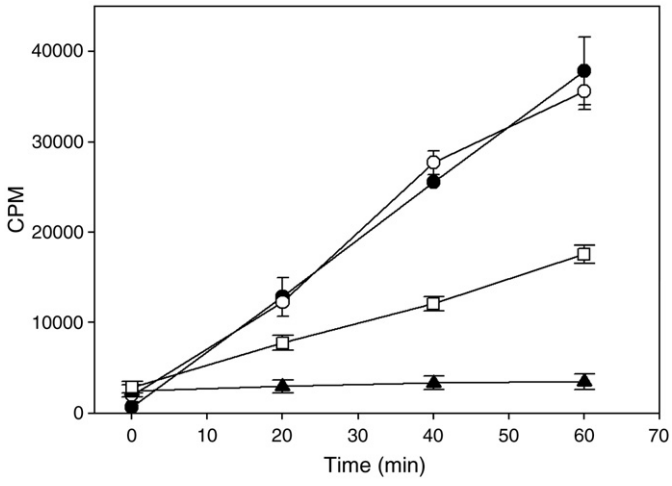

Fig. 4. Effect of 2,4 DNP on the inhibition of RNA synthesis by MccJ25. The incorporation of [^{3}H]uridine by *E. coli* AB1133 was studied as described in Materials and methods. Symbols are (●): control cells, (□):10 μM MccJ25, (○):10 μM MccJ25 plus 200 μM 2,4 DNP, (▲): 10 mM azide. Data are means from three independent experiments with vertical bars representing standard deviation of the means.

Table 2
Rates of oxygen consumption in the presence of 2,4 DNP and MccJ25.

	Rates of oxygen consumption (%O_2/mL)	
	None	2,4 DNP (200 μM)
E. coli AB1133	1.117 ± 0.080[a]	1.818 ± 0.060
E. coli AB1133 + MccJ25	1.090 ± 0.010	1.468 ± 0.026

[a] The results are expressed as mean ± SD of five independent experiments.

was indirectly assayed by measuring the *in vivo* incorporation of [^{3}H] uridine. As it can be seen in Fig. 4, 200 μM 2,4 DNP prevented the inhibition of transcriptional activity in *E. coli* AB1133 cells treated with 10 μM MccJ25.

Next, we compared the activity of MccJ25 on the respiratory chain when the peptide uptake was inhibited by 2,4 DNP. As was previously shown, MccJ25 alone slightly inhibited oxygen consumption in *E. coli* cells. On the other hand, 200 μM 2,4 DNP induced a nearly 2-fold increase of the oxygen consumption (Table 2). Interestingly, the decrease in the rate of bacterial oxygen consumption induced by MccJ25 was higher in the presence of 2,4 DNP compared to cells treated with MccJ25 alone.

The fluorescein-labeled MccJ25 variant at 20 μM final concentration produced the same effects, in the absence and in the presence of 200 μM 2,4 DNP (data not shown).

3.5. ROS overproduction induced by MccJ25 in the presence of 2,4 DNP

Previous work from our laboratory has provided convincing evidences that ROS are produced upon MccJ25 interaction with the respiratory chain [9]. In order to test whether the higher oxygen consumption rates observed upon 2,4 DNP treatment could be increasing the ROS production induced by MccJ25, we explored the intracellular oxidation of the ROS-sensitive fluorescent probe COOH-H_2DCFDA. Probe-loaded bacteria kept at 37 °C under stirring were treated with 2,4 DNP for 15 min. When MccJ25 was added, a steep rise of the fluorescence emission could be seen. The increased magnitude was found to be MccJ25-dose dependent. When MccJ25 was added to control cells without 2,4 DNP, a less pronounced increase of COOH-H_2DCFDA fluorescence emission could be observed (Fig. 5). MccJ25-induced ROS production could be reverted by ascorbic acid. The fluorescence of the probe-loaded cells dropped to basal levels when 10 mM of ascorbic acid were added in the absence of 2,4 DNP. However, in the case of 2,4 DNP-treated cells, the higher increase of fluorescence emission of COOH-H_2DCFDA produced by MccJ25 could not be totally reverted by ascorbic acid, confirming that higher amounts of reactive species have been produced. It is also important to highlight that KCN greatly decreased ROS production upon addition of the antibiotic peptide. Fluorescein oxidation by ROS was also enhanced in the presence of the protonophore CCCP (Fig. 5 inset), indicating that dissipation of the proton motive force contributes to the overproduction of the deleterious species induced by MccJ25 and it is not a specific 2,4 DNP effect. Moreover, increased oxygen consumption rates were also observed in CCCP-treated cells (data not shown), strongly suggesting that this is a common protonophore mechanism of action rather than a specific one.

Production of ROS induced by fluorescein-labeled MccJ25 I13K could not be assayed as the fluorescence emission of the peptide and the ROS-sensitive probe overlapped with each other and saturated the spectrofluorimeter detector. Therefore, no reliable fluorescence intensity changes could be retrieved from the experiments.

4. Discussion

In order to construct a traceable derivative of MccJ25 for peptide incorporation studies in living cells, a lysine carrying variant peptide (MccJ25 I13K) was obtained and purified, and further labeled with the free-amine reactive probe FITC. The I13K variant was shown to retain MccJ25-like structure in a previous work from Severinov et al. [21]. Also, we decided to work with this peptide because the substitution did not lie in the lactame ring zone, which was demonstrated to be important for the transcriptional inhibition activity [9,21,22]. Although the fluorescent peptide turned out to be less potent than native MccJ25, the antimicrobial spectrum as well as the mechanisms of action appeared to be identical: similar inhibition rates were observed for both oxygen consumption and purified RNA polymerase activity, irrespective if either MccJ25 or fluorescein-labeled MccJ25-I13K were used in the assays.

The uptake of labeled peptide was enhanced in FhuA-overexpressing cells, confirming the role of FhuA in the intracellular accumulation of MccJ25 [23–25]. Also, this result suggested us that the fluorescent probe added to MccJ25-I13K produced a small perturbation on the microcin structure because, according to existing evidence, the β-hairpin structure is recognized by FhuA and is important in the bacterial uptake mechanism. Thus, the fluorescent variant of MccJ25 was used thereafter throughout the work as a peptide that shared both structural and functional properties with MccJ25.

The 80% inhibition of MccJ25 intracellular accumulation upon 2,4 DNP treatment confirmed that MccJ25 uptake is indeed a proton motive force-driven process. The remaining 20% of uptake that was seen in de-energized cells occurred even at the shortest time assayed. A similar rate of uptake was seen in FhuA mutant cells. These results are suggestive of a passive partition of the peptide to bacterial membranes or into bacterial cells. In this paper, peptide binding to membranes of *E. coli* AB1133 was confirmed by ultracentrifugation. The labeled peptide co-sedimented with bacterial membranes prepared by sonication as well as membrane vesicles prepared by spheroplast lysis, either in the absence or in the presence of 2,4 DNP. Moreover, the fluorescein-labeled peptide transferred fluorescence energy by resonance to RhoPE-containing vesicle, further supporting the location of the peptide at the membrane. The energy transfer between the fluorophores was not affected by 2,4 DNP, indicating that the binding to membrane was not impaired, as opposed to the

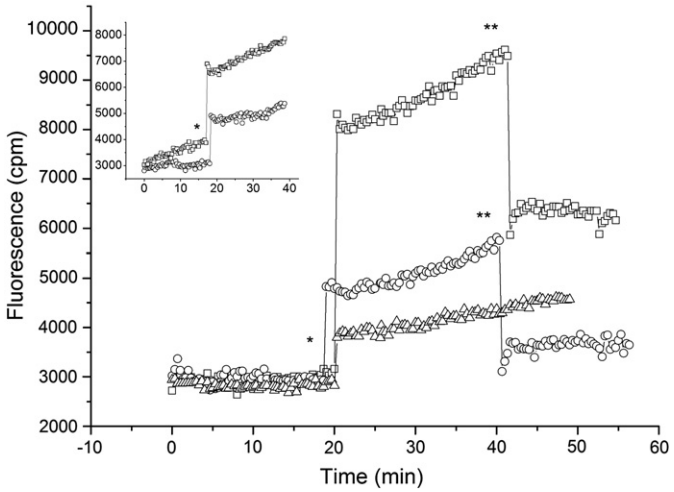

Fig. 5. Effect of 2,4 DNP on the MccJ25-induced ROS generation. The production of ROS was followed by the fluorescence increase of COOH-H_2DCFDA as described in Materials and methods. The *E. coli* AB1133 was preincubated with 5 μM COOH-H_2DCFDA in darkness at 37 °C for 30 min in buffer 20 mM Tris–HCl, pH 7.8, 80 mM NaCl, 1 mM EDTA. Bacterial cells (○) and bacterial cells preincubated 15 min with 200 μM 2,4 DNP (□) or preincubated 15 min with 1 mM KCN (△) were added. Asterisks denote addition of 10 μM MccJ25 (*) and 10 mM ascorbic acid (**). λ_{ex}: 490 nm, λ_{em}: 520 nm). Inset: Effect of the protonophore CCCP on the MccJ25-induced ROS generation in AB1133 cells. Control cells without CCCP (○) and preincubated 15 min with 1 mM CCCP (□) were treated with 10 μM MccJ25.

diminished intracellular accumulation. Actually, the bacterial transcriptional activity assayed in this work, which is executed by cytoplasmic target of MccJ25, the RNA polymerase enzyme, could not be inhibited by the peptide when the cells were treated with the protonophore. As antimicrobial activity of MccJ25 showed minor changes in the presence of 2,4 DNP, in spite of the drastic inhibition of intracellular accumulation of the peptide and the absence of transcriptional activity inhibition as well, the peptide binding to plasma membrane in an energy-independent manner might be involved in the observed antimicrobial activity.

Bellomio et al. [9] proved that superoxide anion was produced as a consequence of MccJ25 interaction with the enzymes of the respiratory chain. Herein, by measuring the fluorescence emission of cells loaded with the ROS-sensitive probe COOH-H_2DCFDA, an oxidative burst was detected upon interaction of MccJ25 with cells. The ROS-sensitive probe was oxidized at higher rates when AB1133 cells were treated with MccJ25 in the presence of either 2,4 DNP or CCCP. The ROS scavenger agent ascorbic acid induced a complete recovery of the fluorescence emission in the absence but not in the presence of the protonophores. A fluorometric assay of bacterial transmembrane potential indicated that both CCCP and 2,4 DNP were able to transiently dissipate it, as cells treated with either protonophore were able to restore the $\Delta\Psi$ (data not shown). The results suggest that cells increase electron flow through the respiratory chain (Table 2) in order to maintain the membrane potential in spite of the constant proton leakage. On the other hand, MccJ25 diminished the oxygen consumption rates of cells treated with either 2,4 DNP or CCCP; moreover, this inhibition was higher than that observed with cells treated with MccJ25 and no protonophore. Taken together, these results strongly suggest a general mechanism of action where MccJ25 takes advantage of the protonophore-enhanced electron flow to induce the generation of ROS. Intriguingly, in other systems such as mitochondria, an uncoupling effect is generally associated with decreased ROS formation. However, in MccJ25-treated bacteria there is no net uncoupling since cells are able to compensate for it as discussed above. Indeed, in cells incubated with MccJ25 and DNP there is a 1.3-fold increase in oxygen consumption. Therefore, ROS production is truly favoured.

Lethal properties of ROS and their role in the mechanism of action of bactericidal antibiotics were also observed in different kind of bactericidal but not bacteriostatic antibiotics in a previous work by Kohanski et al. [26]. The deleterious oxidative radical species were generated inside cells as a consequence of a metabolic depletion of NADH and iron–sulphur clusters destabilization.

However, our results suggest that ROS are produced as a consequence of a direct interaction of this antimicrobial peptide with some component(s) of the plasma membrane, presumably a respiratory chain-related protein. Interestingly, cyanide pre-treatment greatly inhibited MccJ25 effect suggesting that respiratory chain terminal oxidases are likely to be the target of MccJ25. In this regard, Bellomio et al. [9] reported that cyanide addition prevented the inhibition of respiratory enzymes induced by MccJ25, which is in agreement with our present findings. Also, the increased electron flow through the respiratory chain induced by 2,4 DNP in an attempt of cells to restore proton gradient can be related to the overproduction of ROS induced by MccJ25. This overproduction of deleterious species may account for the antimicrobial activity that is observed in the absence of RNA polymerase inhibition. Indeed, only the effective plasma membrane concentration rather than total MccJ25 intracellular concentration correlated with the antimicrobial activity of MccJ25. In this regard, MccJ25 was reported to inhibit NADH and succinate dehydrogenase and alter the oxygen consumption rate in *Salmonella enterica* serovars [8] as well as inhibit the mitochondrial complex III [27]. This alternative pathway may account for the bactericidal properties of the peptide and it would deserve great attention for improving the antibiotic activity of MccJ25.

Acknowledgments

This work was supported by Consejo Nacional de Investigaciones Científicas y Técnicas (CONICET, Argentina), Agencia de Promoción Científica y Tecnológica (FONCYT, Grants PICTO 843/04 and PAE 22642) and Secretaria de Ciencia y Técnica de la Universidad Nacional de Tucumán (CIUNT, Grant D313). R.D.M. and C.J.M. are Career Investigators of CONICET. F.G.D. and M.V.N.C. are recipients of CONICET fellowships. We are deeply indebted to Dr Valentinuzzi for his helpful assistance in writing this manuscript.

References

[1] M.J. Bayro, J. Mukhopadhyay, G.V.T. Swapna, et al., Structure of antibacterial peptide microcin J25: a 21-residue lariat protoknot, J. Am. Chem. Soc. 125 (2003) 12382–12383.
[2] K. Adelman, J. Yuzenkova, A.L. Porta, et al., Molecular mechanism of transcription inhibition by peptide antibiotic Microcin J25, Mol. Cell 14 (2004) 753–762.
[3] K.J. Rosengren, R.J. Clark, N.L. Daly, U. Göransson, A. Jones, D.J. Craik, Microcin J25 has a threaded sidechain-to-backbone ring structure and not a head-to-tail cyclized backbone, J. Am. Chem. Soc. 125 (2003) 12464–12474.
[4] K.-A. Wilson, M. Kalkum, J. Ottesen, et al., Structure of microcin J25, a peptide inhibitor of bacterial RNA polymerase, is a lassoed tail, J. Am. Chem. Soc. 125 (2003) 12475–12483.
[5] R.A. Salomon, R.N. Farias, Microcin 25, a novel antimicrobial peptide produced by *Escherichia coli*, J. Bacteriol. 174 (1992) 7428–7435.
[6] J. Mukhopadhyay, E. Sineva, J. Knight, R.M. Levy, R.H. Ebright, Antibacterial peptide microcin J25 inhibits transcription by binding within and obstructing the RNA polymerase secondary channel, Molecular Cell 14 (2004) 739–751.
[7] M.A. Delgado, M.R. Rintoul, R.N. Farias, R.A. Salomon, *Escherichia coli* RNA polymerase is the target of the cyclopeptide antibiotic microcin J25, J. Bacteriol. 183 (2001) 4543–4550.
[8] M.R. Rintoul, B.F.d. Arcuri, R.A. Salomon, R.N. Farias, R.D. Morero, The antibacterial action of microcin J25: evidence for disruption of cytoplasmic membrane energization in *Salmonella newport*, FEMS Microbiol. Lett. 204 (2001) 265–270.
[9] A. Bellomio, P.A. Vincent, B.F.d. Arcuri, R.N. Farías, R.D. Morero, Microcin J25 Has dual and independent mechanisms of action in *Escherichia coli:* RNA polymerase inhibition and increased superoxide production, J. Bacteriol. 189 (2007) 4180–4186.
[10] R.E.d. Cristóbal, J.O. Solbiati, A.M. Zenoff, et al., Microcin J25 Uptake: His5 of the MccJ25 lariat ring is involved in interaction with the inner membrane MccJ25 transporter protein SbmA, J. Bacteriol. 188 (2006) 3324–3328.
[11] J.O. Solbiati, M. Ciaccio, R.N. Farias, R.A. Salomon, Genetic analysis of plasmid determinants for microcin J25 production and immunity, J. Bacteriol. 178 (1996) 3661–3663.
[12] M.R. Rintoul, B.F.d. Arcuri, R.D. Morero, Effects of the antibiotic peptide microcin J25 on liposomes: role of the acyl chain length and the negatively charged phospholipid, Biochim. Biophys. Acta 1509 (2000) 65–72.
[13] I. Yamato, Y. Anraku, K. Hirosawa, Cytoplasmic membrane vesicles of *Escherichia coli*. A simple method for preparing the cytoplasmic and outer membranes, J. Biochem. 77 (1975) 705–718.
[14] T. Tsuchiya, Oxidative phosphorylation in right-side-out membrane vesicles from *Escherichia coli*, J. Biol. Chem. 251 (1976) 5315–5320.
[15] A.P. Singh, P. Nicholls, Cyanine and safranine dyes as membrane potential probes in cytochrome *c* oxidase reconstituted proteoliposomes, J. Biochem. Biophys. Methods 11 (1985) 95–108.
[16] L.A. Schurig-Briccio, M.R. Rintoul, S.I. Volentini, et al., A critical phosphate concentration in the stationary phase maintains *ndh* gene expression and aerobic respiratory chain activity in *Escherichia coli*, FEMS Microbiol. Lett. 284 (2008) 76–83.
[17] S.M. Colles, G.M. Chisolm, Lysophosphatidylcholine-induced cellular injury in cultured fibroblasts involves oxidative events, J. Lipid Res. 41 (2000) 1188–1198.
[18] J. Yuzenkova, M.A. Delgado, S. Nechaev, et al., Mutations of bacterial RNA polymerase leading to resistance to microcin J25, J. Biol. Chem. 277 (2002) 50867–50875.
[19] G.S. Moeck, J.W. Coulton, TonB-dependent iron acquisition: mechanisms of siderophore-mediated active transport, Mol. Microbiol. 28 (1998) 675–681.
[20] A. Bellomio, R.G. Oliveira, B. Maggio, R.D. Morero, Penetration and interactions of the antimicrobial peptide, microcin J25, into uncharged phospholipid monolayers, J. Colloid Interface Sci. 285 (2005) 118–124.
[21] O. Pavlova, J. Mukhopadhyay, E. Sineva, R.H. Ebright, K. Severinov, Systematic structure-activity analysis of microcin J25, J. Biol. Chem. 283 (2008) 25589–25595.
[22] E. Semenova, J. Yuzenkova, J. Peduzzi, S. Rebuffat, K. Severinov, Structure–activity analysis of microcin J25: distinct parts of the threaded lasso molecule are responsible for interaction with bacterial RNA polymerase, J. Bacteriol. 187 (2005) 3859–3863.
[23] D. Destoumieux-Garzón, S. Duquesne, J. Peduzzi, et al., The iron-siderophore transporter FhuA is the receptor for the antimicrobial peptide microcin J25: role of

the microcin Val11-Pro16 beta-hairpin region in the recognition mechanism, Biochem. J. 389 (2005) 869–876.
[24] R.A. Salomon, R.N. Farias, The FhuA protein is involved in microcin 25 uptake, J. Bacteriol. 175 (1993) 7741–7742.
[25] R.A. Salomon, R.N. Farias, The peptide antibiotic microcin 25 Is Imported through the TonB pathway and the SbmA protein, J. Bacteriol. 177 (1995) 3323–3325.
[26] M.A. Kohanski, D.J. Dwyer, B. Hayete, C.A. Lawrence, J.J. Collins, A common mechanism of cellular death induced by bactericidal antibiotics, Cell 130 (2007) 797–810.
[27] M.V. Niklison Chirou, C.J. Minahk, R.D. Morero, Antimitochondrial activity displayed by the antimicrobial peptide microcin J25, Biochem. Biophys. Res. Commun. 317 (2004) 882–886.